PHYSICAL REVIEW E **92**, 062512 (2015)

Droplet relaxation in Hele-Shaw geometry: Application to the measurement of the nematic-isotropic surface tension

Patrick Oswald[*] and Guilhem Poy

Université de Lyon, Ecole Normale Supérieure de Lyon, Laboratoire de Physique, CNRS, 46 Allée d'Italie, 69364 Lyon, Cedex 07, France

(Received 16 October 2015; published 22 December 2015)

Shape measurements after the coalescence of isotropic droplets embedded in a thin sample of a homeotropic nematic phase provides a tool to measure the nematic-isotropic surface tension. In addition, this experiment allows us to check the scaling laws recently given by Brun *et al.* [P.-T. Brun, M. Nagel, and F. Gallaire, Phys. Rev. E **88**, 043009 (2013)] to explain the relaxation of ellipsoidal droplets in a Hele-Shaw cell.

DOI: 10.1103/PhysRevE.92.062512 PACS number(s): 61.30.Hn, 68.03.Cd, 47.61.Fg

I. INTRODUCTION

In a recent article, Brun *et al.* [1] studied the relaxation of an ellipsoidal drop of a fluid 1 placed in a Hele-Shaw cell filled with a fluid 2 (Fig. 1). The two fluids are immiscible, of viscosities μ_1 and μ_2, and the surface tension that drives the process is denoted by γ. Fluid 2 is at rest at infinity and wets the walls of the cell. The main result of this theoretical and numerical study is that the drop deformation $D_f = (L - W)/W$ (where L and W denote the drop length and width, respectively) relaxes to 0 exponentially with the typical time constant $\tau_r = \frac{R^3(\mu_1+\mu_2)}{h^2\gamma}$. In this expression R is the final radius of the droplet ($R = \sqrt{WL}/2$) and h is the cell thickness assumed to be small with respect to R. More precisely, Brun *et al.* have shown that

$$D_f(t) = D_f(0)\exp\left(-\alpha\frac{t}{\tau_r}\right), \tag{1}$$

where α is a number (of the order of 0.36) that depends very little on both the confinement ratio $k = R/h$ and the viscosity ratio $r = \mu_1/(\mu_1 + \mu_2)$ (in the limit $4 \leqslant k \leqslant 10$ and $0 \leqslant r \leqslant 10/11$) [1].

These predictions have not yet been checked in microfluidic devices and the reason certainly arises from the difficulty in preparing ellipsoidal droplets of different sizes in a fluid at rest at infinity (although this could be done by submitting for a short time the droplet to a hyperbolic flow [2]). For this reason, we performed this experiment in a different way by observing the coalescence and the relaxation of droplets of isotropic liquid in a homeotropic sample of nematic liquid crystal. This experiment, which was conducted in the coexistence region of the two phases, has several advantages over standard experiments with microfluidic devices: The sample thickness and the droplet radius can be changed very easily and the dynamics is much slower than with a usual liquid because the nematic-isotropic surface tension is 3 to 4 orders of magnitude smaller than that between two usual liquids (such as oil and water).

In addition, the measurement and prediction of the nematic-isotropic surface tension has long attracted attention from both theorists [3–11] and experimentalists [12–15]; hence the interest of proposing an alternative method to measure accurately this quantity.

II. SAMPLE PREPARATION

The liquid crystals (LCs) chosen are two pure compounds, 4-*n*-heptyl-4′-cyanobiphenyl (7CB) (Merck, Germany) [16] and 4α,4′α-propylheptyl-1α,1′α-bicyclohexyl-4β-carbonitrile (CCN37) (Nematel, Germany) [17]. They are used without further purification. The 7CB (CCN-37) LC melts at about 42.65 °C (54.75 °C). Their freezing range at the nematic-isotropic phase transition is of the order of 0.05 °C, which is too small to stabilize the size of the droplets during the experiments. For this reason, we dope them with 5 wt. % of biphenyl (BP) in order to increase their freezing range. For the mixture 7CB + BP (CCN-37 + BP), we measure $T_{\text{solidus}} \approx 34.9\,^{\circ}\text{C}$ and $T_{\text{liquidus}} \approx 35.6\,^{\circ}\text{C}$ ($T_{\text{solidus}} \approx 48.4\,^{\circ}\text{C}$ and $T_{\text{liquidus}} \approx 48.6\,^{\circ}\text{C}$). The samples are prepared between two float glass plates (of size $20 \times 20 \times 1.1$ mm^3) and nickel wires of calibrated diameter are used as a spacer. The sample thickness is always larger than 5 μm, which is much more than the critical thickness, of the order of 0.1 μm [18], below which the substrate ordering starts to shift the transition temperature. The thickness in the center of the sample is measured to within ±0.1 μm with a spectrophotometer before filling with the LC. The parallelism between the glass plates is adjusted while viewing the interference fringes in natural light. Samples with more than two fringes over the whole surface area are systematically eliminated. Polyimide Nissan 0626 and silane ZLI 3124 from Merck are used to achieve strong homeotropic anchoring. With these surface treatments, the nematic phase completely wets the glass plates. Both give similar results. The samples are sealed on the sides with UV glue NOA 81 (Norland Optical adhesive) to prevent the BP from evaporating [19]. The samples are placed inside a homemade oven, the temperature of which is controlled to within ±0.01 °C by a RKC HA400 controller.

III. EXPERIMENTAL RESULTS

To observe the drop coalescence, the sample is slowly heated from the homeotropic nematic phase. Once the temperature is above T_{solidus}, drops of isotropic liquid nucleate in the sample. By moving the sample inside the oven, we look for a pair of drops that are close to each other, but well isolated from the others. The temperature is then increased

---

[*] patrick.oswald@ens-lyon.fr

1539-3755/2015/92(6)/062512(5)

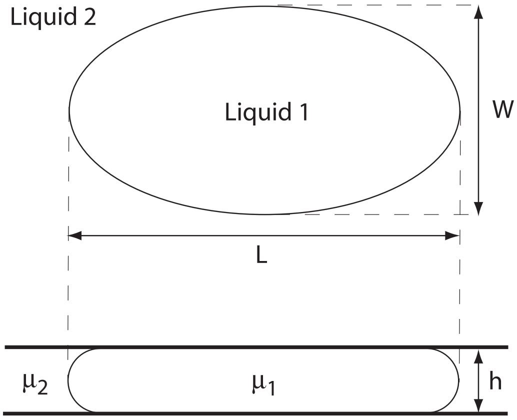

FIG. 1. Drop geometry.

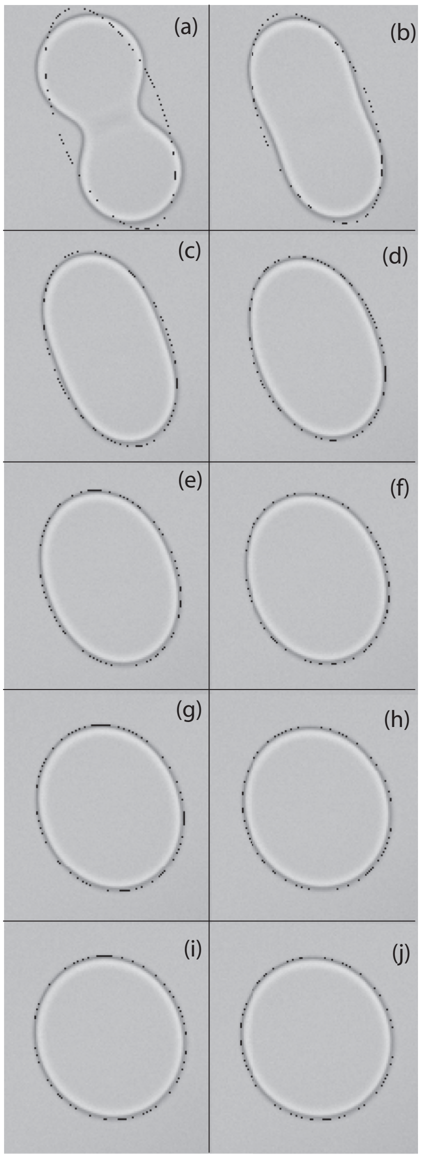

FIG. 2. Relaxation of a drop of isotropic liquid in a homeotropic nematic sample of the mixture 7CB + 5%BP. The time interval between two photos is 4 s. The ellipses in dashed line have been fitted by IMAGEJ. The sample thickness is $h = 9.5$ μm and the final drop radius is $R \approx 45$ μm.

very slowly (by typically 0.02 °C per minute) in order to grow the drops. When they are almost in contact, the temperature is stabilized. After some time, the drops coalesce, forming a single drop. A waist forms that progressively disappears and the drop becomes ellipsoidal before it slowly relaxes to a circular shape.

In this paper we focus our attention on this slow, final relaxation process. An example is shown in Fig. 2. In this example, the photos are taken in natural light and the microscope is slightly defocused in order to better see the side of the droplet. An examination between crossed polarizers shows that the nematic phase remains perfectly homeotropic during the final stage of the relaxation process, once the waist is well formed [as in the photo in Fig. 2(a)]. The situation is different at the very beginning of the coalescence because a short birefringence flash is observed just when the waist forms. This flash shows that the director field transiently destabilizes, but this is beyond the scope of the paper. The images are recorded with a videocamera AVT PIKE F-145B and then treated using the software IMAGEJ. In practice, a threshold is applied to each image to extract the drop contour, which is then fitted to an ellipse. This allows us to measure the deformation D_f of the drop as a function of time. The curve corresponding to the pictures shown in Fig. 2 is shown in Fig. 3 with its fit to an exponential law. The fit is in excellent agreement with the theory of Brun *et al.* [1]. In the following we denote by τ the relaxation time found experimentally. The hydrodynamic theory predicts that $\tau h^2/R^3$ depends only slowly on the confinement ratio $k = R/h$ [see Eq. (1)]. To test this prediction, we measured systematically this quantity as a function of the confinement ratio in samples of different thicknesses (ranging between 5 and 22 μm). Our results are shown in Fig. 4 for the two liquid crystals studied. The data are a bit dispersed. Four reasons can explain this dispersion. First, the droplets are seldom exactly of the same radius when they coalesce. In practice, we took care to keep only pairs of droplets for which the radius difference was lower than typically 10%. In this case, the ellipsoidal shape is rapidly

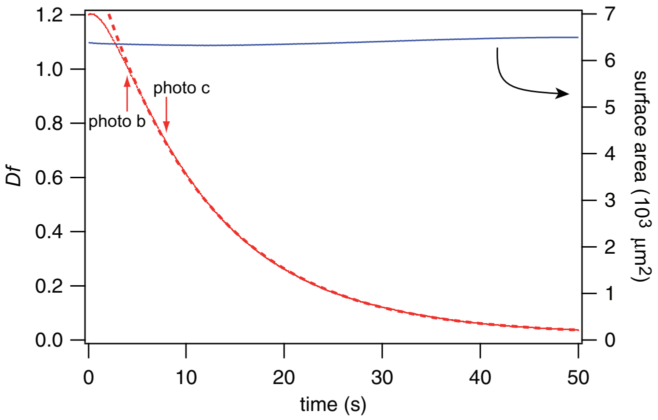

FIG. 3. (Color online) Drop deformation Df and drop surface area as a function of time for the sequence of pictures shown in Fig. 2. The surface area is constant to better than 2% during the whole relaxation process. The dashed line is the best fit of Df to an exponential law. The fit is typically indistinguishable from the experimental curve from the photo in Fig. 2(b).

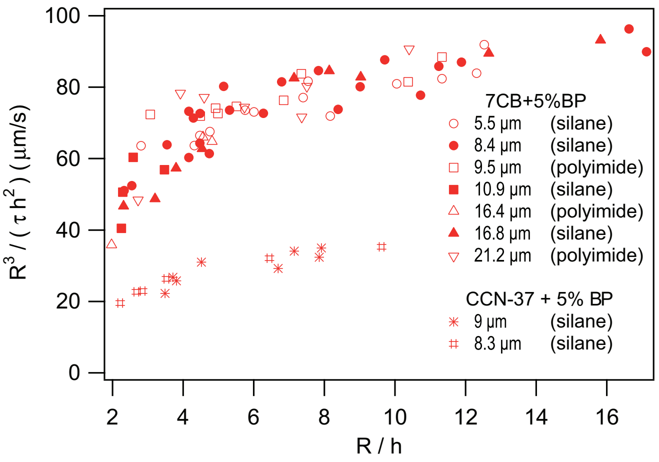

FIG. 4. (Color online) Combination $R^3/\tau h^2$ as a function of the confinement ratio R/h for the two mixtures studied. Note that in these experiments, τ typically varied from 2 to 700 s.

reached as shown in Fig. 2. Second, it is very difficult (but not impossible) to prepare pairs of droplets that are completely isolated from the others. However, we realized that the results were not significantly changed when other drops were present in the vicinity of the relaxing drop, i.e., at a distance of the order of or larger than R. For this reason, we kept these drops in our analysis. Third, the sample thickness can change a little (within an optical fringe) in the central part of the sample observed in the microscope (of size 1×1 cm^2). This means that the thickness is known at best to within ± 0.25 μm, which introduces an error of $\pm 10\%$ in the thinnest samples. Finally, one might worry about the existence of nematic layers wetting the plates inside the drops. This could change the radius of curvature of their meniscus and introduce a systematic error. The answer to this question is given by applying the Gibbs-Thomson equation to the meniscus after equilibration of the drops: $T = T_c + mC_I - \frac{\gamma T_c}{\Delta H}\mathcal{C}$. In this equation T is the actual temperature, T_c is the transition temperature of the pure LC, m is the slope of the liquidus, C_I is the impurity concentration in the isotropic liquid (constant at equilibrium), ΔH is the latent heat, and $\mathcal{C}$ is the curvature of the meniscus, here negative. This relation immediately shows that the actual temperature T is always larger than the equilibrium temperature of the planar front $T_c + mC_I$. As a consequence, a macroscopic wetting layer cannot exist, because it must melt. This shows that only wetting layers of microscopic thickness exist between the glass and the isotropic liquid inside the drops when they are equilibrated. The radius of curvature of the meniscus is thus well equal to $h/2$ in the sample thickness, as assumed in the model of Brun *et al.* [1].

IV. DISCUSSION AND SURFACE TENSION MEASUREMENT

Our experimental results show that the relaxation time τ scales like R^3/h^2 as predicted by the hydrodynamic theory. This shows that the two phases behave as two immiscible fluids. This observation is important because the drop could also relax via a melting-recrystallization process. Nonetheless, this process is very slow and negligible here as it takes a typical time [20]

$$\tau_{\mathrm{mr}} \sim \frac{\Delta H \Delta T}{\gamma T_c D} R^3, \tag{2}$$

independent of h, where T_c is the transition temperature of the pure compound, ΔT the freezing range, ΔH the latent heat per unit volume, and D the diffusion coefficient of the impurity (BP in our case). With typical values $\gamma \approx 10^{-5}$ N/m [12,14], $\Delta H \approx 10^6$ J/m^3 [16], $D \approx 10^{-10}$ m^2/s, $T_c \approx 300$K, $\Delta T \approx 1\,^\circ$C, and $R = 30$ μm, we calculate $\tau_{\mathrm{mr}} \sim 10^5$ s, which is indeed very long with respect to time τ measured experimentally (of the order of 10 s).

Our goal is to measure γ, so we need to know the viscosities of the two phases. Viscosity μ_1 is well defined because it is the viscosity of the isotropic liquid η_{iso}. By contrast, viscosity μ_2 is less clear because, in nematic liquid crystals, the viscosity depends on the orientation of the director $\vec{n}$ with respect to the velocity $\vec{v}$ and the velocity gradient $\vec{\nabla} v$. In our case, the nematic is sheared both in the plane and in the thickness of the sample. For this reason, μ_2 must be a combination of the two Miesowicz viscosities η_a (measured when $\vec{n} \perp \vec{v}$ and $\vec{n} \perp \vec{\nabla} v$) and η_c (measured when $\vec{n} \perp \vec{v}$ and $\vec{n} \parallel \vec{\nabla} v$) [21]. However, we can argue that when $h \ll R$, the viscous dissipation is dominated by the Poiseuille flow in the sample thickness. For this reason, and because the nematic remains perfectly homeotropic during the final stage of the relaxation, we can safely assume that μ_2 is very close to viscosity η_c and take $\mu_1 + \mu_2 = \eta_{\mathrm{iso}} + \eta_c$. We measured these two viscosities to within $\pm 10\%$ with a piezoelectric rheometer. These measurements are described in detail in another paper [22]. For 7CB, we found $\eta_{\mathrm{iso}} = 0.0235$ Pa s and $\eta_c = 0.0352$ Pa s (in very good agreement with the values given by Ananthaiah *et al.* [23]), which give $r \approx 0.4$, and for CCN-37 we found $\eta_{\mathrm{iso}} = 0.027$ Pa s and $\eta_c = 0.039$ Pa s, which also give $r \approx 0.4$. In practice, we measured $\tau = \tau_r/\alpha = \frac{R^3(\mu_1+\mu_2)}{h^2\gamma\alpha}$ [see Eq. (1)], so we need to know α to determine γ. This coefficient was calculated numerically by Brun *et al.* [1] as a function of the confinement ratio k (for $4 \leqslant k \leqslant 10$) and the viscosity ratio r. They found $\alpha = a + bk$ with $a = 0.36$ and $b = 0.005$ for $r \approx 0.4$. Finally, the surface tension can be calculated from our data and the relation $\gamma = \frac{\eta_{iso}+\eta_c}{\alpha}\frac{R^3}{h^2\tau}$ (where $\frac{R^3}{h^2\tau}$ is given in Fig. 4). Figure 5 shows the values of γ deduced from our measurements of drops of confinement radius $4 \leqslant k \leqslant 10$. This graph shows that for the two liquid crystals studied, the values of γ found experimentally are independent of k within the experimental dispersion and are equal on average to

$$\gamma_{7\mathrm{CB}} = 1.12 \pm 0.2\ 10^{-5}\ \mathrm{N/m},$$
$$\gamma_{\mathrm{CCN\text{-}37}} = 0.56 \pm 0.1\ 10^{-5}\ \mathrm{N/m},$$

where the errors have been estimated by including those on the viscosities. We emphasize that the value found for 7CB agrees within the error with that given by Faetti and Palleschi ($\gamma_{7\mathrm{CB}} = 1.8 \pm 0.7\ 10^{-5}$ N/m [14]).

It is also interesting to compare this value with the value predicted from the Landau–Ginzburg–de Gennes model of the

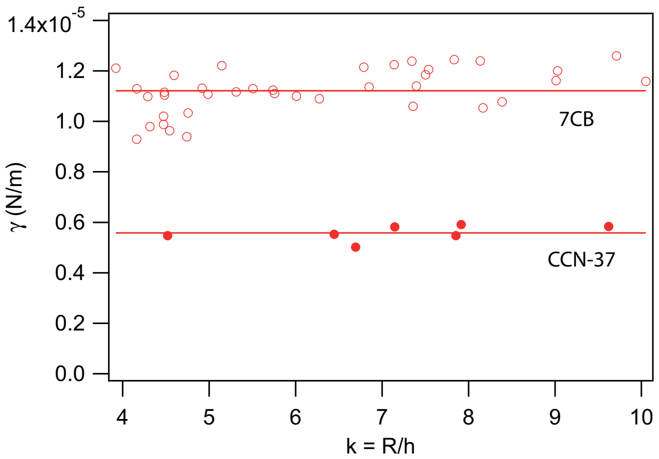

FIG. 5. (Color online) Surface tension γ measured by applying the numerical results of Brun *et al.* [1] as a function of the confinement ratio k when $4 \leqslant k \leqslant 10$.

interface [3,21]

$$\gamma = \frac{2\sqrt{2}}{81}\frac{B^3}{C^2}\sqrt{\frac{L}{C}}, \qquad (3)$$

where B and C are the Landau coefficients for the cubic and quartic terms in the power series expansion of the Landau energy as a function of the quadrupolar order parameter and L is a stiffness coefficient (Ginzburg term). The first two terms have been measured by Coles in 7CB: $B = 3.3 \pm 0.2$ J/cm^3 and $C = 8.1 \pm 0.3$ J/cm^3 [24]. The stiffness L can be estimated from the value of the elastic constant K at the transition by using the relation $K \approx 3LS_c^2$, where $S_c = \frac{2B}{3C}$ is the value of the order parameter at the transition [21]. With $K \approx 2 \times 10^{-12}$ N [25], we obtain $L \approx 9 \pm 3\ 10^{-12}$ N. Finally, we calculate $\gamma = 2 \pm 1\ 10^{-5}$ N/m, which is quite compatible with the measured value. In addition, this model shows that the interface width is equal to the correlation length ξ_c at the transition

$$\xi_c = \frac{3\sqrt{2LC}}{B} \approx 11 \text{ nm}. \qquad (4)$$

This value shows that the interface is sharp at the scale of the droplet that is essential to apply the hydrodynamic model of Brun *et al.* to our system.

To end this section we recall that a disclination line is attached to the meniscus. This line forms because of the existence of a preferential angle between the director and the normal to the interface. This line is attached to the meniscus as shown in directional solidification [26] and has an elastic energy per unit length of the order of $h^2(K/h^2) = K$ independent of h, where K is the Frank constant [27,28]. In our experiments, $K \sim 10^{-12}$ N at the transition [25] and $\pi\gamma h/2 > 10^{-10}$ N so that $\gamma h \gg K$. This shows that the surface tension of the meniscus dominates the line tension of the disclination line (otherwise the scaling law in h^2 for the relaxation time should not apply). Finally, we note that the angle between the director and the normal to the meniscus does not shift significantly from its preferred value because the anchoring penetration length (of the order of 1 μm [29]) is always small with respect to h. This means that we measure in this experiment the equilibrium surface tension.

V. CONCLUSION

In summary, our experiment quantitatively confirms the predictions of the hydrodynamic theory of Brun *et al.* on the drop relaxation in microfluidic channels. This result was obtained by observing the coalescence and the relaxation of drops of isotropic liquid embedded in thin homeotropic nematic samples.

Alternatively, we proposed a convenient method to accurately measure the ratio $\gamma/(\eta_{\text{iso}} + \eta_c)$ and thus the equilibrium surface tension γ, provided the two viscosities are known. We emphasize that this method is easier to use than the sessile drop method employed before [13,14] (which requires very precise measurements of the density of the two phases and needs a much bigger quantity of the liquid crystal). This method is also much more precise than that proposed by Smith [15] and based on the Frenkel relation for the coalescence time τ_c of two spherical drops of same radius R [30]:

$$\tau_c \approx \frac{\eta R}{\gamma}. \qquad (5)$$

The problem with this method is that the Frenkel relation is approximate, involving an average viscosity η badly defined (in particular when the director field inside the drops is distorted, which is always the case in spherical drops), and has difficulty measuring the coalescence time (usually defined as the time at which the waist disappears). For these reason we believe that our method is better suited to accurately measure the nematic-isotropic surface tension.

An extension of this work could be to systematically measure the nematic-isotropic surface tension in liquid crystals doped with impurities (such as polymers or colloids) in order to test recent theoretical predictions about the coupling between the order parameter and impurity concentration profiles at the interface [9,10]. Concerning this point, it seems that the impurity chosen in our work (biphenyl) does not significantly change the surface tension.

ACKNOWLEDGMENT

The authors thank A. Dequidt for useful comments.

---

[1] P.-T. Brun, M. Nagel, and F. Gallaire, Generic path for droplet relaxation in microfluidic channels, Phys. Rev. E **88**, 043009 (2013).

[2] C. Ulloa, A. Ahumada, and M. L. Cordero, Effects of confinement on the deformation of microfluidic drops, Phys. Rev. E **89**, 033004 (2014).

[3] P. G. de Gennes, Short range order effects in the isotropic phase of nematics and cholesterics, Mol. Cryst. Liq. Cryst. **12**, 193 (1971).

[4] H. Kimura and H. Nakano, Statistical theory of surface tension and molecular orientations in nematic liquid crystals.II. The nematic-isotropic interface, J. Phys. Soc. Jpn. **55**, 4186 (1986).

[5] J. Murakami, Molecular theory of surface tension for liquid crystal, J. Phys. Soc. Jpn. **42**, 210 (1977).

[6] Z. Y. Chen and J. Noolandi, Numerical solution of the Onsager problem for an isotropic-nematic interface, Phys. Rev. A **45**, 2389 (1992).

[7] V. Popa-Nita, T. J. Sluckin, and A. A. Wheeler, Statics and kinetics at the nematic-isotropic interface: Effects of biaxiality, J. Phys. (France) II **7**, 1225 (1997).

[8] M. S. Al-Barwani and M. P. Allen, Isotropic-nematic interface of soft spherocylinders, Phys. Rev. E **62**, 6706 (2000).

[9] A. Matsuyama, R. M. L. Evans, and M. E. Cates, Non-uniformities in polymer/liquid crystal mixtures I. interfacial tension, Eur. Phys. J. E **9**, 79 (2002).

[10] V. Popa-Nita and P. Oswald, Surface tension and capillary waves at the nematic-isotropic interface in ternary mixtures of liquid crystals, colloids, and impurities, J. Chem. Phys. **127**, 104702 (2007).

[11] R. Wittmann and K. Mecke, Surface tension of isotropic-nematic interfaces: Fundamental measure theory for hard spherocylinders, J. Chem. Phys. **140**, 104703 (2014).

[12] D. Langevin and M. A. Bouchiat, Molecular order and surface-tension for nematic-isotropic interface of MBBA, deduced from light reflectivity and light-scattering measurements, Mol. Cryst. Liq. Cryst. **22**, 317 (1973).

[13] R. Williams, Measurement of the interfacial tension between nematic and isotropic phases of MBBA, Mol. Cryst. Liq. Cryst. **35**, 349 (1976).

[14] S. Faetti and V. Palleschi, Measurement of the interfacial tension between nematic and isotropic phase of some cyanobiphenyls, J. Chem. Phys. **81**, 6254 (1984).

[15] G. W. Smith, The nematic/isotropic interfacial energy: Determination from the Frenkel relation for droplet coalescence, Mol. Cryst. Liq. Cryst. **102**, 65 (1984).

[16] G. W. Gray, K. J. Harrison, and J. A. Nash, New family of nematic liquid crystals for displays, Electron. Lett. **9**, 130 (1973).

[17] B. S. Scheuble, G. Weber, and R. Eidenschink, Liquid crystalline cyclohexylcarbonitriles: Properties of single compounds and mixtures, Proceedings of the Fourth Display Research Conference on Eurodisplay '84, Paris (http://www.gbv.de/dms/tib-ub-hannover/174122829.pdf, 1984), pp. 65–68.

[18] H. Yokoyama, Nematic-Isotropic Transition in Bounded Thin Films, J. Chem. Soc. Faraday Trans. **84**, 1023 (1988).

[19] P. Oswald and C. Scalliet, Measurement of the dielectric and viscoelastic constants in mixtures of 4,4′-*n*-octyl-cyanobiphenyl and biphenyl, Phys. Rev. E **89**, 032504 (2014).

[20] F. Melo, Dynamique de l'interface smectique A–smectique B en solidification directionnelle, Ph.D. thesis, Ecole Normale Supérieure de Lyon, 1991 .

[21] P. Oswald and P. Pieranski, *Nematic and Cholesteric Liquid Crystals: Concepts and Physical Properties Illustrated by Experiments* (CRC, Boca Raton, 2005).

[22] P. Oswald, Viscoelasticity of a homeotropic nematic slab, Phys. Rev. E **92**, 062508 (2015).

[23] J. Ananthaiah, R. Sahoo, M. V. Rasna, and S. Dhara, Rheology of nematic liquid crystals with highly polar molecules, Phys. Rev. E **89**, 022510 (2014).

[24] H. J. Coles, Laser and electric field induced birefringence studies on the cyanobiphenyl homologues, Mol. Cryst. Liq. Cryst. **49**, 67 (1978).

[25] N.V. Madhusudana and R. Prathiba, Elasticity and orientational order in some cyanobiphenyls: Part IV. Reanalysis of the data, Mol. Cryst. Liq. Cryst. **89**, 249 (1982).

[26] P. Oswald, J. Bechhoefer, and A. Libchaber, Instabilities of a Moving Nematic-Isotropic Interface, Phys. Rev. Lett. **58**, 2318 (1987).

[27] J. Ignés-Mullol, J. Baudry, L. Lejcek, and P. Oswald, Formation of disclination lines near a free nematic interface, Phys. Rev. E **59**, 568 (1999).

[28] O. E. Shklyaev and E. Fried, Interaction between a disclination and a uniaxial-isotropic phase interface in a nematic liquid crystal, J. Colloid Interface Sci. **317**, 298 (2008).

[29] S. Faetti and V. Palleschi, Nematic-isotropic interface of some members of the homologous series of 4-cyano-4′-(*n*-alkyl)biphenyl liquid crystals, Phys. Rev. A **30**, 3241 (1984).

[30] J. Frenkel, Viscous flow of crystalline bodies under the action of surface tension, J. Phys. **9**, 385 (1945).